Article

Lithium-Cation/π Complexes of Aromatic Systems. The Effect of Increasing the Number of Fused Rings

Jean-Franois Gal, Pierre-Charles Maria, Michle Decouzon, Otilia M, Manuel Yez, and Jos Luis M. Abboud

J. Am. Chem. Soc., **2003**, 125 (34), 10394-10401• DOI: 10.1021/ja029843b • Publication Date (Web): 01 August 2003

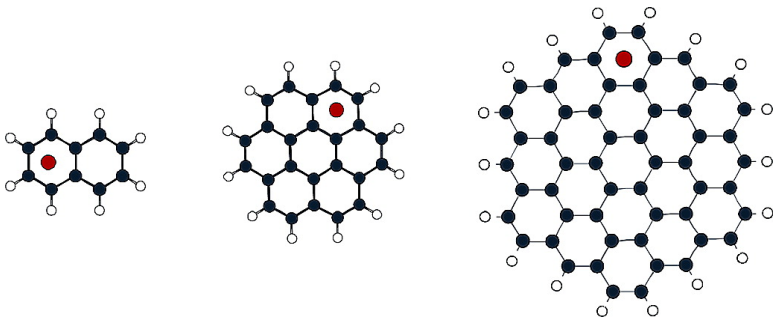

J|A|C|S
ARTICLES
Published on Web 08/01/2003

Lithium-Cation/π Complexes of Aromatic Systems. The Effect of Increasing the Number of Fused Rings

Jean-François Gal,[†] Pierre-Charles Maria,[†] Michèle Decouzon,[†] Otilia Mó,[‡] Manuel Yáñez,*[,‡] and José Luis M. Abboud[§]

Contribution from the Chimie des Matériaux Organiques et Métalliques, Université de Nice-Sophia Antipolis, Parc Valrose, 06108 Nice Cedex 2, France, Departamento de Química, C-9, Universidad Autónoma de Madrid, Cantoblanco, 28049-Madrid, Spain, and Instituto Rocasolano, C.S.I.C., Serrano, 119, 28006-Madrid, Spain

Received December 20, 2002; E-mail: manuel.yanez@uam.es

Abstract: The gas-phase lithium cation basicities (LCBs) of naphthalene, azulene, anthracene, and phenanthrene were measured by means of Fourier transform ion cyclotron resonance (FT-ICR) mass spectrometry. The structures of the corresponding complexes and their relative stabilities were investigated at the B3LYP/6-311+G(3df,2p)//B3LYP/6-31G(d) level of theory. In the theoretical survey, pyrene, coronene, [3]phenylene, angular [3]phenylene, and circumcoronene were also included. The strength of the binding to a given aromatic cycle decreases as the number of cycles directly fused to it increases. Hence, the stability of the outer π-complexes, in which Li^+ is attached to the peripheral rings, is systematically greater than that of the complexes in which the metal is attached to the inner rings. The energy gap between these local minima decreases as the number of fused rings in the system increases. This result seems to indicate that, as the size of the system increases, the rings tend to lose their peculiarities, in such a way that in the limit of a graphite sheet all rings would exhibit identical characteristics and reactivity. The good agreement between calculated LCBs and experimental values lends support to the enhanced stability of the outer complexes. The activation barriers connecting these local minima decrease as the number of fused cycles increases, but seems to tend toward a limit. [3]Phenylene and angular [3]phenylene exhibit enhanced LCBs reflecting nonnegligible Mills−Nixon effects that increase the electron-donor properties of these annelated benzenes.

Introduction

The interest in metal-cation/π complexes has increased significantly in the last two decades as a consequence of the increasing evidence of the participation of this kind of complex in a variety of phenomena, such as biochemical activity, molecular recognition, catalysis, chemistry in condensed phases, etc.

A great deal of attention has been devoted to the particular subset of alkali-metal-cation/π complexes,[1−12] mostly involving benzene and its derivatives.[13−18] Quite surprisingly, there is much less information as far as other extended aromatic compounds are concerned: we are aware of the paper of Pozniak and Dunbar[19] in which the formation of M(coronene)$^+$ and M(coronene)$_2^+$ complexes involving 25 different metal cations has been investigated. Later, Dunbar[20] reported the binding of metal ions to planar and curved surfaces by comparing the behavior of different metal monocations with coronene and corannulene. Also, very recently, Caraiman and Bohme[21] carried out an investigation of the gas-phase reactivity of iron cations coordinated to benzene and coronene, and Deng et al.[22] reported the formation of endohedral metallofullerenes by collision of K^+ with C_{60} in the gas phase.

One open question is how the extension of the π-face influences the binding of alkali metal cations. Such a study will provide some useful clues for understanding the interactions of these ions with graphitic surfaces. Because the interactions

[†] Université de Nice-Sophia Antipolis.
[‡] Universidad Autónoma de Madrid.
[§] C.S.I.C.

(1) Larrivee, M. L.; Allison, J. *J. Am. Chem. Soc.* **1990**, *112*, 7134.
(2) Goldfuss, B.; Schleyer, P. v. R.; Hampel, F. *J. Am. Chem. Soc.* **1997**, *119*, 1072.
(3) Ma, J. C.; Dougherty, D. A. *Chem. Rev.* **1997**, *97*, 1303.
(4) Cerda, B. A.; Wesdemiotis, C. *Int. J. Mass Spectrom.* **1999**, *189*, 189.
(5) Fujii, T. *Mass Spectrom. Rev.* **2000**, *19*, 111.
(6) McMahon, T. B.; Ohanessian, G. *Chem.-Eur. J.* **2000**, *6*, 2931.
(7) Wu, J.; Polce, M. J.; Wesdemiotis, C. *J. Am. Chem. Soc.* **2000**, *122*, 12786.
(8) Armentrout, P. B.; Rodgers, M. T. *J. Phys. Chem. A* **2000**, *104*, 2238.
(9) Rodgers, M. T.; Armentrout, P. B. *Mass Spectrom. Rev.* **2000**, *19*, 215.
(10) Siu, F. M.; Ma, N. L.; Tsang, C. W. *J. Chem. Phys.* **2001**, *114*, 7045.
(11) Kar, T.; Pattanayak, J.; Scheiner, S. *J. Phys. Chem. A* **2001**, *105*, 10397.
(12) Tsang, Y.; Siu, F. M.; Ma, N. L.; Tsang, C. W. *Rapid Commun. Mass Spectrom.* **2002**, *16*, 229.
(13) Nicholas, J. B.; Hay, B. J. *J. Phys. Chem. A* **1999**, *103*, 9815.
(14) Feller, D.; Dixon, D. A.; Nicholas, J. B. *J. Phys. Chem. A* **2000**, *104*, 11414.
(15) Burk, P.; Koppel, I. A.; Koppel, I.; Kurg, R.; Gal, J.-F.; Maria, P.-C.; Herreros, M.; Notario, R.; Abboud, J.-L. M.; Anvia, F.; Taft, R. W. *J. Phys. Chem. A* **2000**, *104*, 2824.
(16) Amicangelo, J. C.; Armentrout, P. B. *J. Phys. Chem. A* **2000**, *104*, 11420.
(17) Gal, J.-F.; Maria, P.-C.; Decouzon, M.; Mó, O.; Yáñez, M. *Int. J. Mass Spectrom.* **2002**, *219*, 445.
(18) Amunugama, R.; Rodgers, M. T. *Int. J. Mass Spectrom.* **2003**, *222*, 431.
(19) Pozniak, B. P.; Dunbar, R. C. *J. Am. Chem. Soc.* **1997**, *119*, 10439.
(20) Dunbar, R. C. *J. Phys. Chem. A* **2002**, *106*, 9809.
(21) Caraiman, D.; Bohme, D. K. *Int. J. Mass Spectrom.* **2002**, *223*, 411.
(22) Deng, R.; Clegg, A.; Echt, O. *Int. J. Mass Spectrom.* **2002**, *223*, 695.

10.1021/ja029843b CCC: $25.00

involving alkali metal cations such as Li^+ are essentially electrostatic, Li^+ is able to form planetary systems[23] in which the metal orbits around a molecular moiety because the barriers connecting successive minima are very low. The question to be addressed in the present study is how easy is the movement of an alkali metal ion over an aromatic π-system of increasing size.

Hence, the aim of our paper is to provide some experimental and theoretical data in this direction using Li^+ as a useful probe. As models of aromatic systems with extensively conjugated π-clouds, we considered naphthalene, azulene, anthracene, and phenanthrene for which the gas-phase lithium-cation basicity, LCB, defined as the Gibbs free energies of a base B for the process

$$BLi^+ \rightleftharpoons B + Li^+ \qquad (1)$$

was measured by Fourier transform ion cyclotron resonance (FT-ICR) mass spectrometry. The theoretical study included the aforementioned compounds benzo[3,4]cyclobuta[1,2-*b*]biphenylene or [3]phenylene (**3BPh**) and benzo[3,4] cyclobuta[1,2-*a*]biphenylene or angular [3]phenylene (**aBPh**), for which FT-ICR experiments were undertaken but unsuccessful. Pyrene, coronene, and circumcoronene (tripyreno[2,1,10,9,8,7-*defghij*:2′,1′,10′,9′,8′,7′-*nopqrst*:2″,1″,10″,9″,8″,7″-*xyzaib*1*c*1*d*1] trinaphthylene) were not studied experimentally, but were also considered for the theoretical study, as examples of very extended aromatic systems.

Experimental Section

All compounds presented in Table 1 were of commercial origin (Aldrich, Fluka) and of the highest purity available. Samples of **3BPh** and **aBPh** were kindly provided by Pr. Peter Vollhardt. Reactants were introduced in the FT-ICR spectrometer without further purification, except for degassing by several freeze−pump−thaw cycles. The lithium cation was generated by laser ablation (pulsed nitrogen laser, 337 nm, 200 μJ per pulse) from a lithium benzoate target, in the form of a pellet obtained by compression of the salt.[24] In most of the cases, it was not useful to add 2-chloropropane to the systems under scrutiny to generate the propene/Li^+ adduct, which in turn transfers Li^+ to ligands of larger LCB. Equilibrium constants were determined at several (three or more) different pressure ratios. Polycyclic aromatic hydrocarbons (PAH), of low volatility, were introduced in the FT-ICR analyzer with leak valves, allowing a sufficient time (sometimes several hours) for pressure stabilization, before introducing the more volatile reference compounds. Mass spectra of the pure PAH and of the mixtures with the reference were recorded during this introduction step to check for the absence of significant amount of impurities. Partial pressures were measured using a Bayard−Alpert ion gauge (Alcatel BN 111). Gauge readings were corrected for the different sensitivities (relative to nitrogen) of each compound, evaluated according to Bartmess and Georgiadis,[25] using the polarizability calculated by the Miller additivity scheme.[26]

As an example relevant to this study, it is interesting to consider the calculated relative sensitivity for benzene, 4.062, which is fairly close to the experimental value, 4.14 ± 0.18, determined using a spinning rotor gauge (Leybold Viscovac VM 210). Experimental determination of relative sensitivities for PAH was not attempted, considering their low vapor pressures. For the sake of consistency, we relied only on calculated values, including those for reference compounds. Pressure measurements are one of the major sources of error in the equilibrium constant determination. Taking into account random and systematic errors on pressure determinations, uncertainties on equilibrium constants are estimated to be in the 20−30% range, leading to uncertainties on ΔG of 0.5−0.7 kJ mol^{-1}. Other sources of errors, such as secondary reactions, may contribute to augment the overall uncertainty. In fact, the 95% confidence limits concerning the overlap between the experiments carried out for a base of interest with various references, given for LCB(B) in Table 1, ranging from 0.5 to 1.0 kJ mol^{-1}, are a measure of this overall uncertainty. Reaction times of about 10 s were used. As there was no heat source close to the ICR cell (except for the electromagnet poles at about 30 °C, which are external to the vacuum chamber), the experiments were conducted at a temperature close to 25 °C.

Attempts to determine equilibrium constants involving **3BPh** were unsuccessful, due to decomposition in the heated inlet system of the FT-ICR spectrometer. Nevertheless, we observed reversible exchanges with butanal and diethyl ether, showing the LCB of **3BPh** is not far from that (about 140 kJ mol^{-1}) of these compounds (see Table 1). No further experiments were attempted on **aBPh**.

The experimental determination of the LCB for naphthalene, azulene, anthracene, and phenanthrene relied on 16 equilibrium measurements, ΔLCB reported in Table 1. LCBs of the four compounds were inferred from a simultaneous optimization of the overlapping of these experimental data, together with 43 other ΔLCBs previously determined, involving 29 compounds (with increasing LCB) ranging from 2,2,2-trifluoroethanol to di-isopropyl ether (16 reference compounds from ref 15; 6 benzene derivatives presented in ref 24; the 3 alkylbenzenes to be published; and naphthalene, azulene, phenanthrene, anthracene studied here). The 59 ΔLCBs considered were treated by a multiple linear regression procedure, as used by Taft and co-workers[27] following the Free and Wilson treatment.[28] Each experiment (ΔLCB) is described

Table 1. Lithium Cation Basicities (LCBs in kJ mol^{-1} at 373 K) for Benzene, Naphthalene, Azulene, Anthracene, and Phenanthrene

			LCB/kJ mol^{-1}	
compound (B)	reference (ref)	ΔLCB/kJ mol^{-1}	ref[a]	B[a]
	CF_3CH_2OH		110.9[b]	
benzene				114.4 (114.6)[c]
naphthalene	1,4-dioxane	2.50 ± 0.35	125.2	127.7 ± 0.5
	CF_3CO_2Et	1.86 ± 0.12	126.3	
	C_6H_5OMe	1.01 ± 0.05	126.7	
	MeCHO	−2.99 ± 0.17	130.4	
phenanthrene	EtCHO	4.38 ± 0.98	136.3	141.1 ± 0.8
	n-PrCHO	2.77 ± 0.03	139.0	
	Et_2O	0.36 ± 0.14	140.4	
	HCO_2Et	−0.99 ± 0.72	142.1	
anthracene	EtCHO	6.09 ± 0.38	136.3	141.5 ± 1.0
	n-PrCHO	2.37 ± 0.38	139.0	
	Et_2O	0.49 ± 0.07	140.4	
	HCO_2Et	−0.67 ± 0.09	142.1	
azulene	Et_2O	5.46 ± 0.52	140.4	145.1 ± 0.8
	MeCN	2.07 ± 0.31	142.6	
	$(n\text{-Pr})_2O$	−5.13 ± 0.79	150.0	
	Me_2CO	−5.99 ± 0.25	151.1	

[a] Lithium cation basicities (LCBs) for reference compounds (ref) and for aromatic compounds (B) studied here; data were obtained by a Free−Wilson treatment of 59 experimental ΔLCBs, see text; the consistency of the LCB measurements for each B may be checked by calculating LCB(B) = LCB(ref) + ΔLCB for the different ref; when indicated, uncertainties correspond to the 95% confidence limits, based on the overlap between the experiments carried out for the base of interest with the various references. [b] All values are anchored to the experimental LCB of CF_3CH_2OH,[14,26] which is the least basic compound of the series involved in the Free−Wilson treatment. [c] From a previous Free−Wilson treatment including only 52 experiments. [17]

(23) Abboud, J. L. M.; Alkorta, I.; Davalos, J. Z.; Gal, J. F.; Herreros, M.; Maria, P. C.; Mó, O.; Molina, M. T.; Notario, R.; Yáñez, M. *J. Am. Chem. Soc.* **2000**, *122*, 4451.
(24) Herreros, M.; Gal, J. F.; Maria, P. C.; Decouzon, M. *Eur. Mass Spectrom.* **1999**, *5*, 259.
(25) Bartmess, J. E.; Giorgiadis, R. M. *Vacuum* **1983**, *3*, 149.
(26) Miller, K. J. *J. Am. Chem. Soc.* **1990**, *112*, 8533.
(27) Chen, L. Z.; Flammang, R.; Maquestiau, A.; Taft, R. W.; Catalán, J.; Cabildo, P.; Claramunt, R.; J., E. *J. Org. Chem.* **1991**, *56*, 179.

by a series of the presence (1), or absence (0), of LCB intervals, no constant term being included in the model. This led to a model explaining 99.05% of the variation in the experiments.

Theoretical estimates of the temperature effect on LCBs showed that the change in LCB, when going from 298 to 373 K, is nearly constant, ranging from 5.5 to 6.7 kJ mol^{-1}.

Computational Details

Standard density functional theory calculations were carried out using the Gaussian 98 suite of programs.[29] Among the different functionals available, we have chosen the B3LYP method which combines Becke's three-parameter nonlocal hybrid exchange potential[30,31] with the nonlocal correlation functional of Lee, Yang, and Parr[32] because it has a very good performance as far as the description of metal-ion/molecule interactions is concerned. Furthermore, we have also shown that Li^+ binding energies evaluated at the B3LYP/6-311+G(3df,2p) level of theory on B3LYP/6-31G(d) optimized geometries are in very good agreement with FT-ICR experimental values.[17] Hence, this will be the theoretical model adopted for the present study. For the particular case of circumcoronene, the size of the system led us to use the B3LYP/3-21G* level for geometry optimization, the corresponding final energies being obtained by single-point B3LYP/6-31+G(d,p) calculations. In all cases, the harmonic vibrational frequencies were calculated at the same level of theory used in the geometry optimization to classify the different stationary points of the potential energy surface as local minima or transition states and to estimate the zero point energy (ZPE) corrections. These ZPE corrections were scaled by the empirical factor 0.98 proposed by Scott and Radom.[33] The corresponding Li^+ binding enthalpies, LBEs, were evaluated by subtracting from the energy of the complex the energy of the neutral and that of Li^+, after including the zero point energy (ZPE) corrections, as well as the translational, rotational, vibrational, and PV thermal contributions, which were estimated as $(^3/_2)RT$, $(^3/_2)RT$, and RT, respectively. For these corrections, we have used $T = 373$ K, which is the temperature of the reference scale used for the anchoring of our data. The corresponding basis set superposition error (BSSE) was not included because it has been shown to be rather small for ion complexes involving aromatic systems[34] if large basis set expansions are used. Furthermore, to assess that this is indeed the case, we estimated this error for naphthalene−, anthracene−, and pyrene−Li^+ complexes, and it was found to be always smaller than 2.5 kJ mol^{-1}. To convert the calculated binding energies (LBE) into binding free energies (LCB), we used the entropy values calculated from the different translational, rotational, and electronic partition functions as implemented in the Gaussian 98 suite of programs.[29] For those cases such as naphthalene, anthracene, coronene, circumcoronene, etc. where several equivalent binding sites exist, the corresponding statistical corrections are accounted for by means of the appropriate symmetry numbers, following the criteria of Bishop and Laidler,[35] as discussed in a previous publication by one of us.[36] As we shall discuss later, this different statistical weight will have some relevance as far as the distribution of the different isomers of Li^+ complexes is concerned.

To analyze the bonding, we have used the atoms in molecules (AIM) theory.[37] Using this theoretical procedure, we have located the relevant bond critical points as well as the ring critical points associated with each aromatic ring.

Results and Discussion

The optimized equilibrium geometries of Li^+ complexes as well as those of the transition states connecting the different local minima are schematized in Figure 1. The complete sets of optimized geometrical parameters are available from the authors upon request. The total energies, as well as the lithium-cation binding enthalpies (LBE) and lithium cation basicities (LCB), are summarized in Table 2.

Structures and Vibrational Frequencies. As it could be easily anticipated, all of the aromatic systems under scrutiny exhibit a number of local minima for the Li^+ complexes equal to the number of fused rings. However, with the only exception of naphthalene, where both local minima are strictly identical by symmetry, for the remaining compounds there is a nonnegligible stability difference between their Li^+ complexes depending on the relative position of the aromatic ring that directly interacts with the metal cation. We systematically found that the binding energy when the metal cation interacts with the peripheral rings is larger than that when the metal cation is positioned over the inner rings. For instance, the anthracene complex in which Li^+ is attached to the central ring is less stable by 3.5 kJ mol^{-1} than the two minima in which the metal cation interacts with one of the two side rings. A similar trend is observed in the case of coronene. The complex in which Li^+ interacts with the central ring lays 7.9 kJ mol^{-1} higher in energy than the six equivalent minima in which the metal cation is positioned over the peripheral aromatic rings. In the case of pyrene, there is not really a central ring, but we can distinguish two kinds of aromatic rings, those which share two C−C bonds with their neighbors and those which share three C−C bonds. Again, in this case, the former type of rings binds Li^+ slightly more strongly than the latter. Hereafter, we shall name outer complexes those in which Li^+ sits above the more external aromatic rings, and inner complexes those where Li^+ sits above the internal aromatic rings.

To understand the origin of this difference, we have located for all of the systems investigated the corresponding ring critical points (rcp's) (see Table 3). The important finding is that the charge density at these rcp's for the peripheral rings is systematically larger than that for the inner rings, in agreement with the enhanced binding energy calculated for the former. The fact that outer rings are electron richer than inner rings can be easily understood if one takes into account that the former have a larger number of C−H bonds than the latter and that the sp^2 carbon is significantly more electronegative than H. This role of hydrogen atoms has been well established in the literature.[38−41] This should be reflected in a quadrupole moment larger for the outer than for the inner rings. Consistently, the molecular electrostatic potential (MEP) is more attractive above

(28) Free, S. M.; Wilson, J. W. *J. Med. Chem.* **1964**, *7*, 395.
(29) Frisch, M. J.; Trucks, G. W.; Schlegel, H. B.; Scuseria, G. E.; Robb, M. A.; Cheeseman, J. R.; Zakrzewski, V. G.; Montgomery, J. A.; Stratmann, R. E.; Burant, J. C.; Dapprich, S.; Millam, J. M.; Daniels, A. D.; Kudin, K. N.; Strain, M. C.; Farkas, O.; Tomasi, J.; Barone, V.; Cossi, M.; Cammi, R.; Mennucci, B.; Pomelli, C.; Adamo, C.; Clifford, S.; Ochterski, J.; Petersson, G. A.; Ayala, P. Y.; Cui, Q.; Morokuma, K.; Malick, D. K.; Rabuck, A. D.; Raghavachari, K.; Foresman, J. B.; Cioslowski, J.; Ortiz, J. V.; Stefanov, B. B.; Liu, G.; Liashenko, A.; Piskorz, P.; Komaromi, I.; Gomperts, R.; Martin, R. L.; Fox, D. J.; Keith, T.; Al-Laham, M. A.; Peng, C. Y.; Nanayakkara, A.; González, C.; Challacombe, M.; Gill, P. M. W.; Johnson, B.; Chen, W.; Wong, M. W.; Andres, J. L.; González, C.; Head-Gordon, M.; Replogle, E. S.; Pople, J. A. *Gaussian 98*, revision A.3; Gaussian, Inc.: Pittsburgh, PA, 1999.
(30) Becke, A. D. *Phys. Rev. A: Gen. Phys.* **1988**, *38*, 3098.
(31) Becke, A. D. *ACS Symp. Ser.* **1989**, *394*, 165.
(32) Lee, C.; Yang, W.; Parr, R. G. *Phys. Rev. B: Condens. Matter* **1988**, *37*, 785.
(33) Scott, A. P.; Radom, L. *J. Phys. Chem.* **1996**, *100*, 16502.
(34) Zhu, W.-L.; Tan, X.-J.; Puah, C. M.; Gu, J.-D.; Jian, H.-L.; Chen, K.-X.; Felder, C. E.; Silman, I.; Sussman, J. L. *J. Phys. Chem. A* **2000**, *104*, 9573.
(35) Bishop, D. M.; Laidler, K. J. *J. Chem. Phys.* **1965**, *42*, 1688.
(36) Catalán, J.; Abboud, J.-L. M.; Elguero, J. *Adv. Heterocycl. Chem.* **1987**, *41*, 187.
(37) Bader, R. F. W. *Atoms in Molecules. A Quantum Theory*; Clarendon Press: Oxford, 1990.

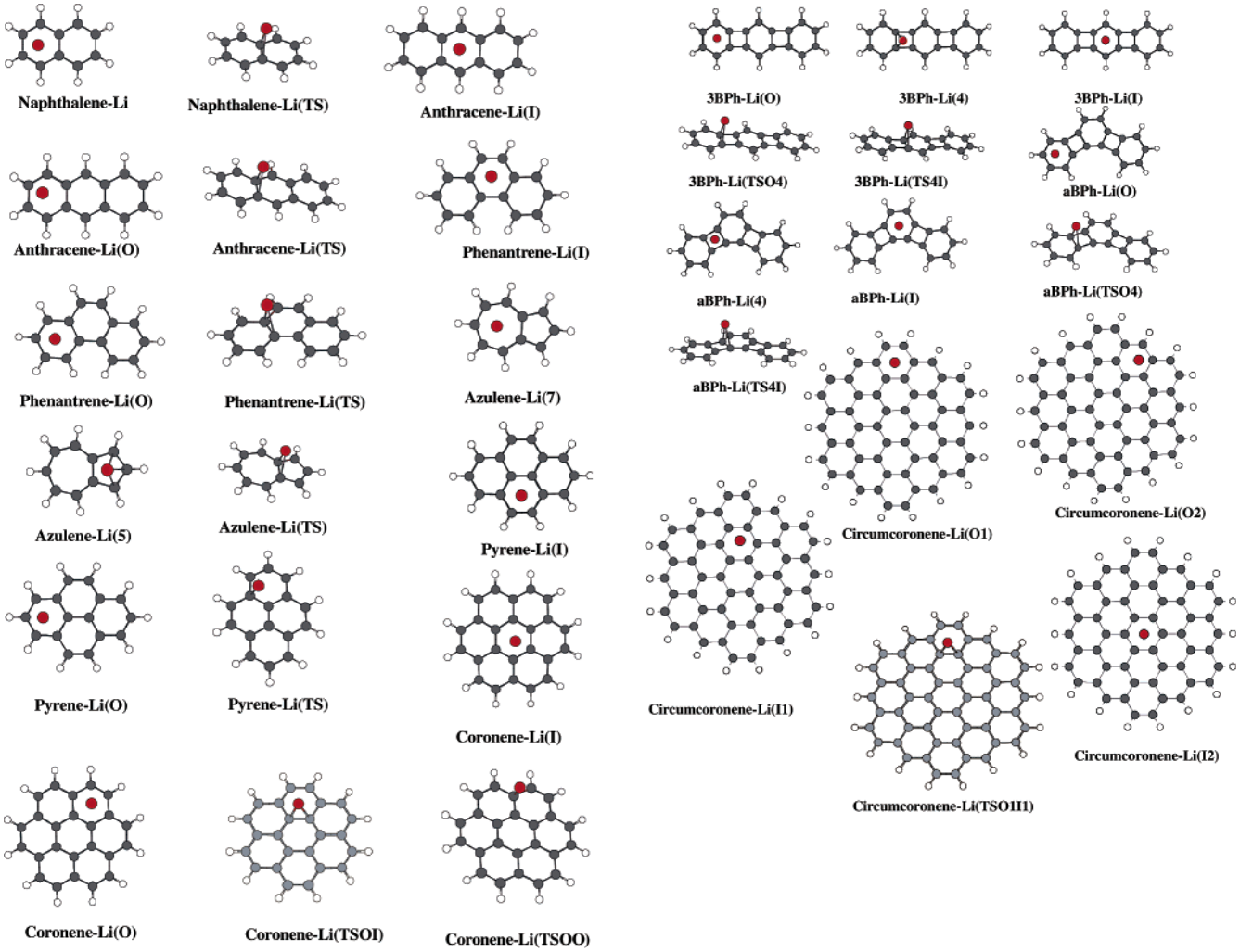

Figure 1. Structures of Li^+ complexes of different aromatic compounds and the transition states connecting the different local minima.

the outer than above the inner rings. This is illustrated in Figure 2 for the particular cases of anthracene, phenanthrene, pyrene, and coronene. For coronene, for example, it is apparent that the negative region of the MEP (with contour values of the potential lower than −0.010 au) has a hole over the inner ring. On the other hand, it must be taken into account that nonelectrostatic terms, such as the polarizability of the aromatic, are also important. Yet also the outer rings behave as better electron donors than the inner rings. This is clearly mirrored on the net charge of Li within the complex. As expected, this net charge, evaluated using the NBO partition technique,[42] is slightly smaller than unity, but the important point is that the amount of charge transferred is systematically larger when the metal interacts with outer rings (0.048 vs 0.032 e^-, respectively). Concomitantly, the net positive charge of the hydrogens belonging to the ring interacting with the metal is systematically larger (about 0.02 e^-) than that of the hydrogen atoms of the ring(s) noninteracting with the metal cation. This actually explains why for pyrene, where strictly speaking inner rings do not exist, the complexes in which Li^+ interacts with rings that present three C−H bonds are more stable than those in which the interaction involves aromatic rings with only two C−H linkages. The different strength of the interaction is also reflected in the distance between the metal cation and the plane that contains the aromatic ring. These distances are typically about 1.8−1.9 Å (1 Å = 0.1 nm), but they are 0.02 Å shorter, in average, for outer than for inner complexes. Also consistently, and in agreement with what has been previously found for a large set of benzene derivatives−Li^+ complexes,[17] all of the complexes investigated exhibit a vibration in the region 380−400 cm^{-1} (see Table 4), which corresponds to the vertical displacement of the metal cation with respect to the aromatic ring ($\nu_{ring-Li}$). More importantly, this stretching vibration appears at higher frequencies for those complexes in which Li^+ interacts with the peripheral aromatic rings, reflecting a greater force constant.

It is also worth noting that the outer complexes can be considered entropically favored, because they are systematically less symmetric than the inner complexes. For instance, for the particular case of anthracene, even if the outer and the inner complexes would have the same LBE, which is not the case, there should be an equilibrium mixture of 66% of the outer and 33% of the inner complexes.

Stabilization of Li^+ adducts and proton adducts (i.e., protonated forms of these hydrocarbons) seems to be determined by

(38) Schleyer, P. v. R. *NATO Adv. Study Inst. Ser. C* **1986**, *189*, 69.
(39) Hamilton, J. G.; Plake, W. E. *J. Am. Chem. Soc.* **1993**, *115*, 4159.
(40) Johnson, W. T. G.; Borden, W. T. *J. Am. Chem. Soc.* **1997**, *119*, 5930.
(41) Alcamí, M.; Mó, O.; Yáñez, M. *J. Comput. Chem.* **1998**, *19*, 1072.
(42) Weinhold, F. In *Encyclopedia of Computational Chemistry*; Schleyer, P. v. R., Allinger, N. L., Clark, T., Gasteiger, J., Kollman, P. A., Schaefer, H. F., III, Schreiner, P. R., Eds.; John Wiley & Sons: Chichester, U.K., 1998; Vol. 3, p 1792.

Table 2. Total Energy (E, hartrees), Relative Energy (ΔE, kJ mol^{-1}), Zero Point Energy (ZPE, hartrees), Entropy (S, cal mol^{-1}), Li^+ Binding Enthalpy (LBE, kJ mol^{-1}), and Lithium Cation Basicity (LCB, kJ mol^{-1}) for Different Aromatic Derivatives

	B3LYP/6-31G*			B3LYP/6-311+G(3df,2p)			
system[a]	E	ZPE	S	E	ΔE[g]	LBE[h]	LCB[h]
naphthalene	−385.89273	0.14781	81.945	−386.01614		169	128
naphthalene−Li	−393.24873	0.15035	87.257	−393.36703	0.0		
naphthalene−Li(TS)	−393.23878	0.14953	86.879	−393.35642	24.2		
anthracene	−539.53052	0.19455	94.923	−539.69856		179[j]	139[j]
anthracene−Li(O)	−546.89042	0.19702	100.324	−547.05321	−3.5		
anthracene−Li(I)	−546.88075	0.19618	100.501	−547.04276	0.0		
anthracene−Li(TS)	−546.89042	0.19702	100.300	−547.05321	21.1		
phenanthrene	−539.53865	0.19482	95.141	−539.70668		180[j]	140[j]
phenanthrene−Li(O)	−547.89893	0.19745	100.287	−547.06181	−6.8		
phenanthrene−Li(I)	−547.89636	0.19717	100.975	−547.05909	0.0		
phenanthrene−Li(TS)	−547.88806	0.19654	100.356	−547.05023	20.6		
pyrene	−615.77313	0.29768	97.235	−615.95969		184	143
pyrene−Li(O)	−623.13459	0.21020	102.542	−623.31611	−9.4		
pyrene−Li(I)	−623.13107	0.20995	103.093	−623.31242	0.0		
pyrene−Li(TS)	−623.12324	0.20937	102.421	−623.30416	18.9		
coronene	−921.89789	0.28028	115.163	−922.16660		186	145
coronene−Li(O)	−929.26108	0.28255	120.755	−929.52339	−7.9		
coronene−Li(I)	−929.25748	0.28234	121.233	−929.52031	0.0		
coronene−Li(TSIO)	−929.25166	0.28193	120.109	−929.51348	15.6		
coronene−Li(TSOO)	−929.25048	0.28190	120.561	−929.51280	18.2		
circumcoronene	−2057.49381[e]	0.53518[e]	178.056[e]	−2069.02034[f]		205[f]	164[f]
circumcoronene−Li(O1)	−2064.82202[e]	0.53688[e]	183.733[e]	−2076.38309[f]	−6.2[f]		
circumcoronene−Li(O2)	−2064.82337[e]	0.53690[e]	183.701[e]	−2076.38386[f]	−8.2[f]		
circumcoronene−Li(I1)	−2064.82207[e]	0.53680[e]	184.021[e]	−2076.38064[f]	0.0[f]		
circumcoronene−Li(I2)	−2064.82206[e]	0.53681[e]	184.015[e]	−2076.38063[f]	0.0[f]		
circumcoronene−Li(TSO1I1)	−2064.81379[e]	0.53628[e]	183.584[e]	−2076.37341[f]	17.7[f]		
azulene	−385.83816	0.14654	85.230	−395.96234		189	147
azulene−Li(5)[b]	−393.20345	0.14945	88.222	−393.32111	−29.2		
azulene−Li(7)[c]	−393.19051	0.14862	89.556	−393.30946	0.0		
azulene−Li(TS)	−393.18907	0.14842	87.568	−393.30704	4.3		
3BPh	−691.81635	0.21623	108.543	−692.02351		192	150
3BPh−**Li**(O)	−699.18069	0.21863	113.556	−699.38278	−9.4		
3BPh−Li(I)	−699.17650	0.21853	113.864	−699.37921	0.0		
3BPh−Li(4)[d]	−699.16956	0.21799	116.373	−699.36985	24.0		
3BPh−Li(TSO4)	−699.16746	0.21771	113.578	−699.36899	0.8[i]		
3BPh−Li(TS4I)	−699.16875	0.21774	113.292	−699.36900	2.2[i]		
aBPh	−691.82039	0.21654	108.307	−692.02736		206	165
aBPh−Li(O)	−699.18542	0.21887	113.528	−699.38785	−7.5		
aBPh−Li(I)	−699.18296	0.21901	113.241	−699.38503	0.0		
aBPh−Li(4)[d]	−699.17652	0.21847	115.636	−699.37776	18.7		
aBPh−Li(TSO4)	−699.17234	0.21806	112.973	−699.37380	7.6		
aBPh−Li(TS4I)	−699.17614	0.21821	112.500	−699.37750	0.7[i]		
Li$^+$			31.798	−7.284918[k]			

[a] O and I designate the outer and inner Li^+ complexes (see text). TS designates the transition state between the local minima. [b] Minimum in which Li^+ sits above the five-membered ring. [c] Minimum in which Li^+ sits above the seven-membered ring. [d] Minimum in which Li^+ sits above the four-membered ring. [e] Values obtained at the B3LYP/3-21G* level. [f] Values obtained at the B3LYP/631+G(d,p)//B3LYP/3-21G* level. [g] These values are always referred to the interior complex and include the corresponding ZPE correction, unless otherwise stated. [h] These values were obtained assuming that only the outer complex would be present in the gas phase, except for those cases where Li^+ complexes are a mixture of inner and outer complexes (see text). [i] These values do not include the ZPE correction. [j] Values obtained assuming that the Li^+ complexes are an equilibrium mixture of exterior and interior complexes (see text). [k] The energy at the B3LYP/6-31+G(d,p) level is −7.28459 hartrees.

Table 3. Charge Density (in au) at the Ring Critical Point of the Aromatic Compounds under Study

	O[a]	I[b]
naphthalene	0.0194	0.0194
anthracene	0.0192	0.0190
phenanthrene	0.0197	0.0184
pyrene	0.0195	0.0188
coronene	0.0192	0.0185
azulene	0.0451[c]	0.0084[d]
3BPh	0.0205	0.0203
aBPh	0.0206	0.0203

[a] O stands for outer ring. [b] I stands for inner ring. [c] Value associated with the five-membered ring. [d] Value associated with the seven-membered ring.

two different mechanisms. Protonated forms are mostly stabilized by the ability of the hydrocarbon framework to delocalize positive charge. At variance with this, Li^+ adducts are mostly stabilized by electrostatic and polarization interactions[3,43] between the cation and the electron-rich regions of the molecules. This is clearly shown in the following cases: (a) The first example is azulene, a nonalternant hydrocarbon endowed with a modest but noticeable dipole moment[44] with an electron-rich five-membered ring. Indeed, our results show that the charge density at the five-membered ring critical point is much larger than that at the seven-membered ring critical point (see Table 3). Accordingly, the interaction is much stronger when Li^+ interacts with the five-membered ring. This stronger electrostatic interaction results also in shorter distances between the metal

(43) Alcamí, M.; Mó, O.; De Paz, J. J. G.; Yáñez, M. *Theor. Chim. Acta* **1990**, *77*, 1.
(44) Abboud, J.-L. M.; Auhmani, A.; Bitar, H.; El Mouhtadi, M.; Martin, J.; Rico, M. *J. Am. Chem. Soc.* **1987**, *109*, 1332.

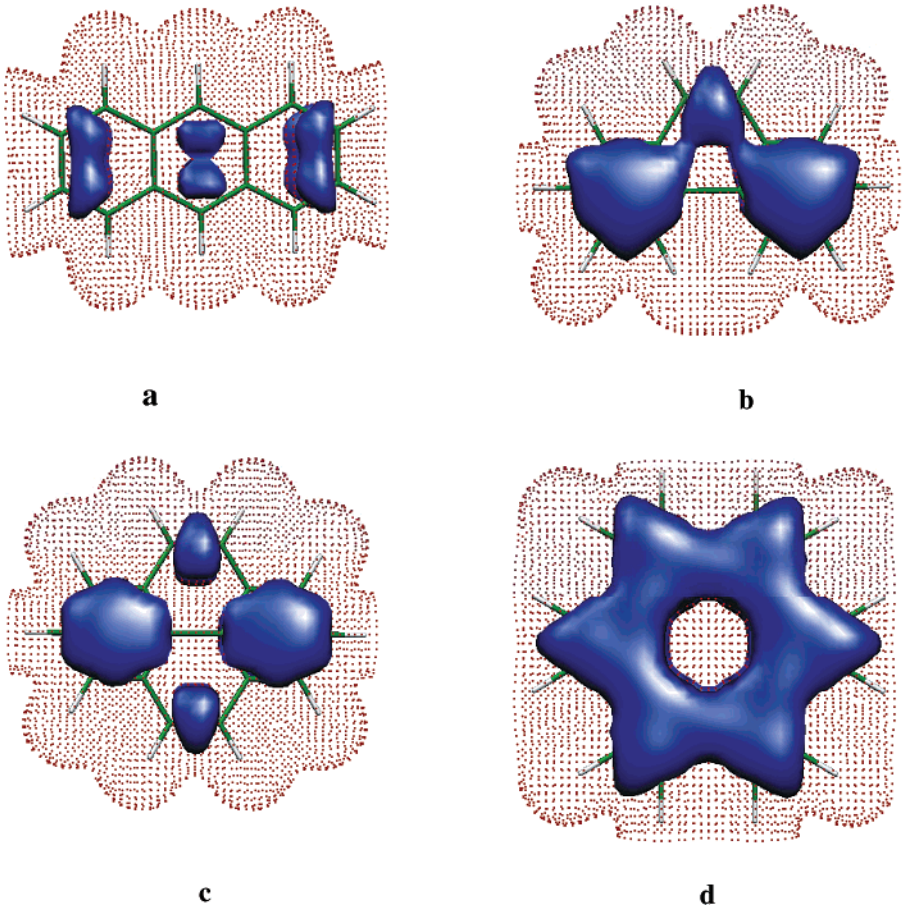

Figure 2. Three-dimensional plot of the molecular electrostatic potential of (a) anthracene, (b) phenanthrene, (c) pyrene, and (d) coronene. The dotted red surface corresponds to positive values of the potential (repulsive regions), whereas the blue lobes correspond to regions where the potential is negative (attractive).

cation and the five-membered ring, leading to larger polarization effects, mirrored in a large charge transfer (0.31 e^-) toward the metal cation, and to an enhancement of the stability of the complex.

(b) The annelated benzene derivatives (series **3BPh** and **aBPh**), classical examples of Mills−Nixon species, are the second example.[45−48] Mills−Nixon effects are associated with the distortions caused on aromatic systems when fused to saturated or to small strained rings. In these two cases, three different local minima are found for the Li^+ complexes. Again, the most stable complex is the one in which the metal cation interacts with the external benzene ring, whereas the less stable corresponds to that in which Li^+ sits above the four-membered ring. However, the relevant finding is that the presence of the four-membered cycle results in a strong localization of the negative charge in the exo bonds of the six-membered rings that facilitate electrophilic attack, in accord with the expectation of the Mills−Nixon effect. As a matter of fact, the charge density at the benzenoid ring critical points of both **3BPh** and **aBPh** is larger than that found for the other compounds here investigated (see Table 3). Consistently, both **3BPh** and **aBPh** exhibit enhanced LBEs. These results seem to be consistent with the unique electron-donor properties reported in the literature[46] for tris-annelated benzenes.

For circumcoronene−Li^+, there exist four nonequivalent local minima, two of which are inner (I1 and I2) and two of which are outer (O1 and O2) complexes (see Figure 1). Our B3LYP/6-31G* estimates indicate that again the outer complexes are 6−8 kJ mol^{-1} lower in energy than the inner complexes. This result seems to indicate that the difference between outer and inner complexes remains sizably large as the size of the system increases. However, the two outer complexes are very close in energy, and the same applies to the two inner, which are practically degenerate. This means that, whereas in coronene the stability difference between inner and outer complexes was about 8 kJ mol^{-1}, for the coronene moiety inside the circumcoronene this difference vanishes. This result seems to indicate that as the size of the system increases the rings tend to lose their peculiarities, in such a way that in the limit of a graphite sheet all rings would exhibit practically identical characteristics and reactivity.

For fused-ring aromatic derivatives, the formation of both outer and inner complexes implies a sizable polarization of the aromatic π-electron density. Consequently, there is a nonnegligible charge transfer from the base toward the Li^+ cation, which in the complex has a net charge of +0.73 au, on average. The withdrawing of charge from the π-cloud results in a slight weakening of all of the C−C bonds of the aromatic rings, which accordingly lengthen by 0.01 Å, on average.

(45) Mills, W. H.; Nixon, I. G. *J. Chem. Soc.* **1930**, 2510.
(46) Rathore, R.; Lindeman, S. V.; Kumar, A. S.; Kochi, J. K. *J. Am. Chem. Soc.* **1998**, *120*, 6012.
(47) Mó, O.; Yáñez, M.; Eckert-Maksic, M.; Maksic, Z. B. *J. Org. Chem.* **1995**, *60*, 1638.
(48) Alkorta, I.; Elguero, J. *Struct. Chem.* **1997**, *8*, 189.

Table 4. Ring−Li^+ Stretching Frequency ($\nu_{ring-Li}$, cm^{-1}) and Out-of-Plane C−H Bending Frequencies (ν_{C-H}, cm^{-1}) for Aromatic Derivatives and Their Li^+ Complexes

system[a]	$\nu_{ring-Li}$	ν_{C-H}
naphthalene		804, 853, 900, 947, 964, 985, 994
naphthalene−Li^+	403	836, 879, 921, 985, 1001, 1014, 1029
anthracene		746, 759, 776, 783, 851, 872, 893, 920, 958, 963, 989
anthracene−Li^+ (O)	405	868, 896, 912, 927, 931, 984, 996, 1007, 1019
anthracene−Li^+ (I)	401	868, 881, 915, 932, 986, 990, 1022
phenanthrene		726, 752, 768, 805, 832, 879, 885, 936, 951, 969, 986
phenanthrene−Li^+(O)	401	765, 878, 810, 846, 889, 910, 966, 987, 990, 1008, 1016
phenanthrene−Li^+(I)	379	767, 792, 858, 879, 900, 972, 983, 1000, 1020, 1022
pyrene		729, 763, 788, 821, 849, 866, 899, 915, 965, 972, 984
pyrene−Li^+(O)	403	781, 796, 831, 837, 877, 926, 943, 992, 1000, 1014
pyrene−Li^+(I)	389	779, 781, 826, 844, 881, 930, 944, 997, 1001, 1015
coronene		777, 780, 800, 821, 858, 879, 950, 958, 969, 977
coronene−Li^+(O)	408	794, 824, 827, 834, 875, 893, 975, 983, 992, 996, 1002
coronene−Li^+(I)	382	796, 831, 87, 900, 982, 989, 1000, 1006
azulene		732, 747, 787, 798, 883, 937, 980, 997, 1007
azulene−Li^+(5)	448	769, 821, 827, 903, 947, 1011, 1034, 1048
azulene−Li^+(7)	362	782, 821, 846, 907, 982, 998, 1009, 1021

[a] O and I stand for outer and inner complexes, respectively.

In addition, in agreement with previous findings,[17] there is a blue-shifting of all of the out-of-plane C−H bending modes upon Li^+ attachment. Again, this frequency displacement is slightly larger for those complexes in which Li^+ sits above the most external rings (see Table 4).

Lithium Cation Basicities. The calculated LBE and LCB values reported in Table 2 were obtained by taking into account that, in some particular cases, the gap between the Gibbs free energies of the outer and the inner complexes is small enough as to ascertain that the least stable complex is present in the gas phase in a significant proportion. Indeed, from our calculated values for the Gibbs energies at 298 K, the anthracene−Li^+ complexes should form an equilibrium mixture of 82% of the outer and 18% of the inner complexes. For phenanthrene, the proportion would be 90% of the outer and 10% of the inner complex, while for pyrene, coronene, circumcoronene, **3BPh**, and **aBPh**, practically only the outer complexes should be observed in the gas phase.

For azulene, only the complex in which Li^+ interacts with the five-membered ring should be observed in the gas phase. This seems to be confirmed by the good agreement between the theoretical LCB, obtained assuming that this is indeed the case, and the experimental LCB. For the remaining systems for which the LCB has been measured, there is also a good agreement between experimental and calculated values. Hence, we may safely assume that our theoretical estimates for the LCB of pyrene, coronene, **3BPh**, and **aBPh** would be reliable.

It is worth mentioning in this respect that the protonic gas-phase basicities of linear polynuclear aromatic hydrocarbons (PAHs) increase very rapidly with the number of rings, roughly reflecting the ability of these systems to disperse positive charge. A combination of experimental and computational data allows one to estimate the limiting basicity of an infinitely long chain.[49] The LCBs of the alternant PAHs also show a dependence on the number of rings and the topology of their arrangement. Here, however, effects are smaller, and although both the LBE and the LCB increase as the number of fused rings increases, as a consequence of the parallel increase in the polarizability of the system, the changes in the LCBs with the size of the system are relatively small. Hence, coronene is found to be slightly more basic than pyrene, whereas pyrene is slightly more basic than anthracene and phenanthrene. The latter two compounds present an almost identical basicity, which, in turn, is larger than that of naphthalene. It can be observed that both **3BPh** and **aBPh** have LCBs larger than aromatic compounds with a similar number of benzene rings, such as phenanthrene and anthracene, and even larger than pyrene or coronene, pointing to unique electron-donor properties of these annelated benzenes. As mentioned above, the distortion on the charge density of the aromatic systems when fused to strained small cycles, associated with the so-called Mills−Nixon effect, is reflected in a larger electron-donor ability, which is in perfect agreement with the findings of Rathore et al.[46] who showed that tris-annelated benzenes exhibit highly reversible oxidation potentials, reflecting nonnegligible Mills−Nixon effects.

Activation Barriers between Outer and Inner Complexes. One of the goals of our work was also to estimate how easy is the displacement of Li^+ from minimum to minimum and how this is affected by the number of fused aromatic rings in the system. For this purpose, we located the corresponding transition states, whose total and relative energies were also included in Table 2. For the sake of consistency, we shall discuss the value of the activation barrier on going from the less stable to the most stable isomer, that is, from inner to outer complexes. The first conspicuous fact is that these energy barriers are about one-fifth of the binding energy of the complex. The second important finding is that the barrier height decreases as the number of fused rings in the system increases. Hence, while for naphthalene this barrier is 25 kJ mol^{-1}, for coronene it is almost one-half this value (15.6 kJ mol^{-1}).

Again, azulene is an exception. Because of the relatively low stability of the complex in which Li^+ is attached to the seven-membered ring, the transition state between this minimum and that in which Li^+ sits above the five-membered ring lies only 4.3 kJ mol^{-1} higher in energy. Something similar happens when considering the **3BPh** and **aBPh** complexes. In this case, the evolution from the less stable local minimum, that is, that in which Li^+ interacts with the four-membered ring, toward any of the other two minima appears to be barrierless when thermal corrections are taken into account, because the estimated barrier is lower than the difference between the zero point energies of the minima and the transition state. Hence, to go from the inner complex to the outer one, the system has to overpass a barrier equal to the stability difference between the inner complex and that in which Li^+ sits above the four-membered ring (20 kJ mol^{-1}). Once this position is reached, the system collapses to the outer complex.

For circumcoronene, we have located the transition state between one of the outer complexes, E1, and the neighbor inner one, I1. The corresponding activation barrier is rather similar to that estimated for the case of coronene (see Table 2). This

(49) Notario, R.; Abboud, J.-L. M. *J. Phys. Chem. A* **1998**, *102*, 5290.

seems to indicate that, although the barrier decreases on going from naphthalene to coronene, the effect of the size of the system on the height of the barrier reaches a limit value, which in our estimates is around 16−18 kJ mol^{-1}.

There is still an interesting question about the mobility of Li^+ ions intercalated between two graphite sheets. In this respect, it is important to note that the typical distance from Li^+ to the aromatic ring is close to one-half of the plane−plane distance (3.35 Å), so the simultaneous interaction with both parallel aromatic systems would result in rather small energy barriers to mobility. However, it must be taken into account that in graphite each sheet is displaced with respect to those lying above and below. Hence, a definite answer to this question would require a more detailed investigation, which is out of the scope of this paper.

Conclusions

From our results on the LCB and LBE of a series of aromatic compounds with different numbers and kinds of fused rings, we can conclude that the binding to a given aromatic cycle within one of these compounds decreases as the number of neighbor cycles directly fused to it increases. More generally, as the number of carbon atoms shared by the ring with its neighbors increases, LCB decreases. Hence, the stability of the outer π-complex, in which Li^+ is attached to the peripheral rings, is systematically greater than that of the complex in which the metal is attached to the inner rings. The energy gap between these local minima changes slightly, as the number of fused rings in the system increases. The good agreement between calculated lithium-cation basicities and experimental values lends support to the enhanced stability of the outer complexes. The activation barriers connecting outer and inner local minima decrease steadily on going from naphthalene to coronene. However, the fact that for coronene and circumcoronene these barriers are practically equal seems to indicate that when the system has reached such a size the barrier reaches a limit. This value is low enough (around 17 kJ mol^{-1}) as to conclude that in the limit of a single graphite sheet, the Li^+ cation will move freely over the surface, at least at temperatures of 600 K or above. As the size of the system increases, the inner rings tend to lose their peculiarities, in such a way that the limit of a graphite sheet is already attained for circumcoronene, where all inner rings exhibit identical characteristics and reactivity. [3]Phenylene and angular [3]phenylene exhibit enhanced LBEs, reflecting nonnegligible Mills−Nixon effects that increase the electron-donor properties of these annelated benzenes.

Acknowledgment. This work has been partially supported by DGI Project Nos. BQU2000-0245 and BQU2000-1497, by the Picasso Project HF2000-0040, and by the COST Action D26. A generous allocation of computational time at the CCC of the Universidad Autónoma de Madrid is also gratefully acknowledged. We thank Peter Vollhardt for samples of [3]phenylenes, and Mary Rodgers for communicating results in advance of publication.

JA029843B